Optimization of Elution Conditions of Chitosan Gel and the Study of Its Adsorbent Mechanism

Zhen-Xing Tang, Jun-Qing Qian, Lu-E Shi

College of Pharmaceutical Science of Zhejiang University of Technology, Hangzhou, Zhejiang 310014, China

Received 26 December 2005; accepted 23 May 2006
DOI 10.1002/app.25327
Published online in Wiley InterScience (www.interscience.wiley.com).

ABSTRACT: Chitosan gel was prepared by crosslinking method. To make use of chitosan gel, the optimization of elution conditions and the adsorbent characteristics of chitosan gel were discussed in this article. The optimum elution conditions were c (NaCl) = 0.05 mol/L in Tris-HCl (pH, 9.05) at the flow rate of 2.0–3.0 mL/min with chitosan gel (particle sizes, 120–140 μm). The effects of contact time, pH, initial BSA concentration, and temperature on adsorption were studied. The equilibrium data could be described well by Langmuir, Freundlich, and Redlich–Peterson models. Adsorption dynamics had been successfully studied by Langergren, intraparticle diffusion model and Avrami model. The thermodynamics parameters ΔG°, ΔH°, and ΔS° were calculated. The spectra studies indicated that the interaction between gel and protein was chiefly through electrostatic attraction in the shape of hydrogen bond. J Appl Polym Sci 103: 1495–1506, 2007

Key words: chitosan; gel; elution; kinetic

INTRODUCTION

Gel has been widely used for protein/enzyme separation in food and pharmaceutical industry.[1] At present, most of the gel carrier is sepharose such as sepharose CL-4B and sepharose CL-6B, which are made by Pharmacia Co. However, sepharose has some drawbacks. First, it is very expensive. Second, the preparation and regeneration of the gel are very difficult. Thus it is significant to produce a new gel, whose price is low and the preparation and regeneration of which are comparatively easy.

Chitosan has many excellent chemical properties similar to sepharose, such as chemical stability and compatibility with bioactive compounds. So it is possible to be used as gel carrier. Homle et al.[2] studied chitosan grafted 1-β-D-furan, using chitosan gel to separate protein, the separation effect of which was not good. Stenstad and Mattiasson[3] used chitosan as gel, but chitosan and the objective protein was difficult to be separated. Shi et al. prepared two kinds of affinity gel, the separation results of which were not effective too.[4]

The amine groups in chitosan molecule are able to adsorb metals through several mechanisms, including chemical interactions such as chelation, electrostatic interactions such as ion exchange, or the formation of ion pairs.[5–7] The kind of interaction depends on the metal, sorbent chemistry, and solution pH.[6–11] Chitosan has also been studied for cadmium removal using raw material[12,13] and derivatives produced by physical and/or chemical modifications.[14–17]

To make use of chitosan gel, the elution conditions of chitosan gel and its adsorbent mechanism were investigated in this work.

EXPERIMENTAL

Materials

Chitosan was provided by Yuhuan Ocean Biochemical Co. (Zhejiang, China); Deacetylation degree of Chitosan was 87%; Glutaraldehyde (25%) was purchased from Wulian Chemical Factory (Shanghai, China); Bovine Serum Albumin (BSA) was purchased from Huamei Bio-Chemical Factory (Zhejiang, China); All other reagents used were of analytical grade and purchased from local suppliers.

Preparation of chitosan gel

A certain amount of chitosan was dissolved in 2.0% acetic acid (v/v) and filtered to remove insoluble materials. The dissolved chitosan was extruded into 2.0% (w/v) NaOH solution with a thin nozzle. Then chitosan was washed with distilled water repeatedly until it was neutral. Chitosan, distilled water, and glutaraldehyde (25%) were added into a flask for cross-

Correspondence to: J.-Q. Qian (qjq@zjut.edu.cn).

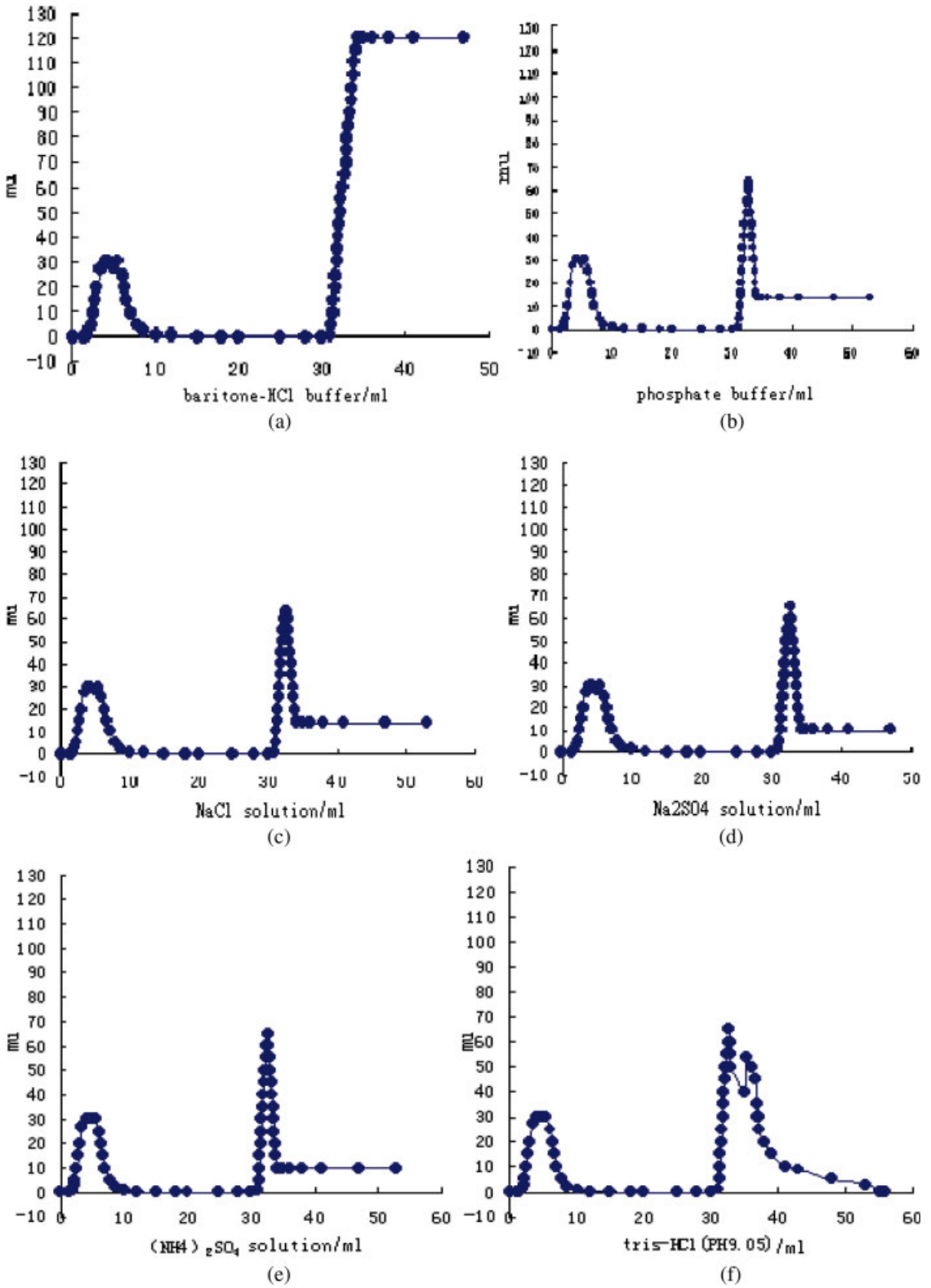

Figure 1 Elution curve under different elution systems. [Color figure can be viewed in the online issue, which is available at www.interscience.wiley.com.]

linking. This procedure was carried out for 6 h at room temperature. Then 20 mL $NaBH_4$ (1.0%, w/v) was added. And the mixture was stirred for 24 h. This gel was filtered and thoroughly rinsed with distilled water until it was neutral. After the gel was sifted by sieving, different sizes of chitosan gel were got.

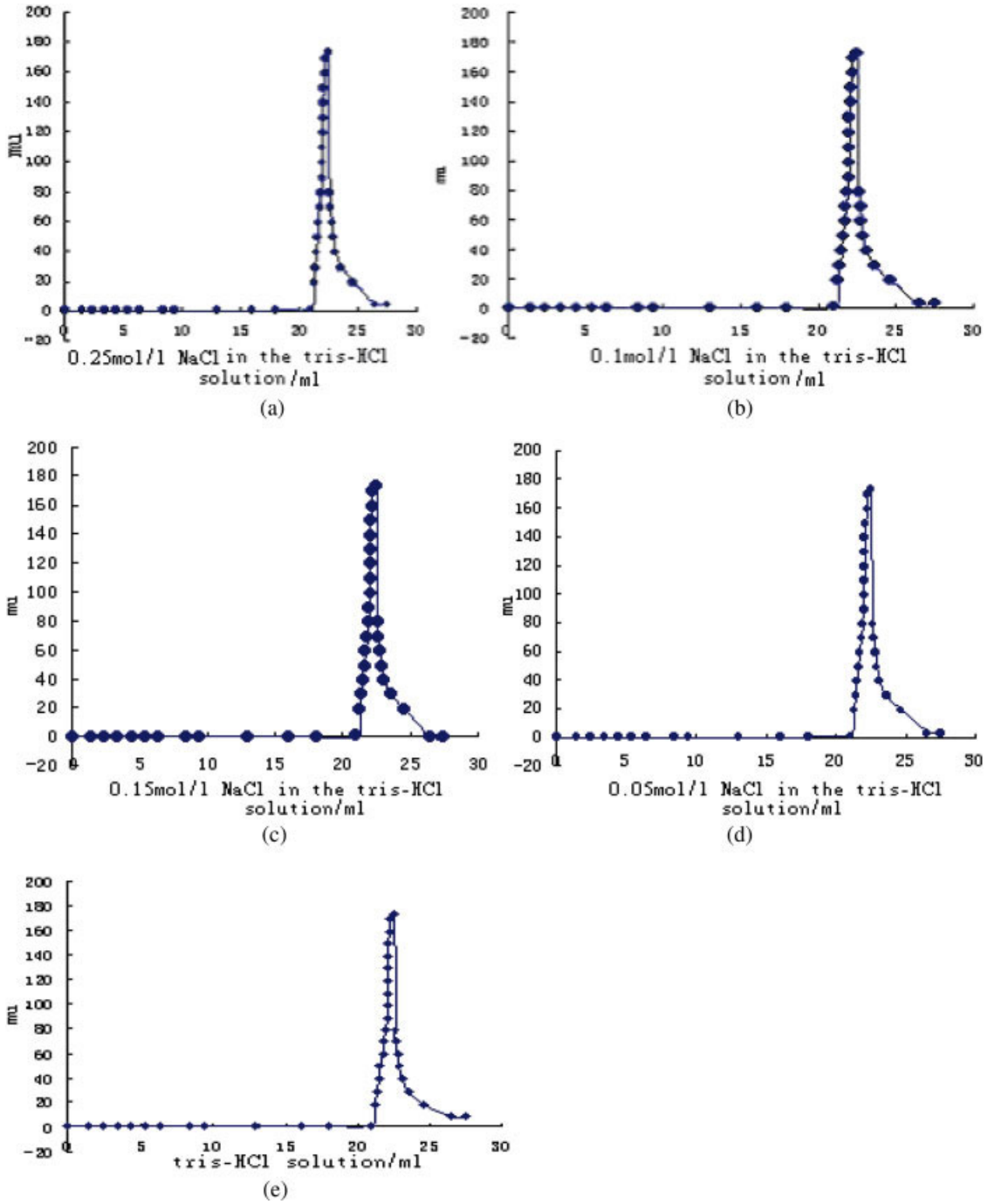

Figure 2 Effect of ion strength on elution conditions. [Color figure can be viewed in the online issue, which is available at www.interscience.wiley.com.]

Determination of elution system

Chitosan gel to be examined was packed into a column (10 mm* 300 mm). The settled chitosan gel was equilibrated with distilled water. BSA was dissolved in distilled water, whose concentration was 20 mg/mL. The BSA sample (1.0 mL) was loaded. The elution system was NaCl (0–0.50 mol/L), Tris-HCl (pH, 9.05), $(NH_4)_2SO_4$ (0–0.50 mol/L), phosphate buffer (pH, 8.0), baritone-HCl (pH, 9.0) respectively. The elution process was examined all the time by nucleic acid and protein detecting machine (Shanghai, China). The eluate was collected by fractional collector machine (Shanghai, China).

Optimization of elution conditions

Chitosan gel was packed and equilibrated. The BSA sample (20 mg/mL, 1.0 mL) was loaded. Using the

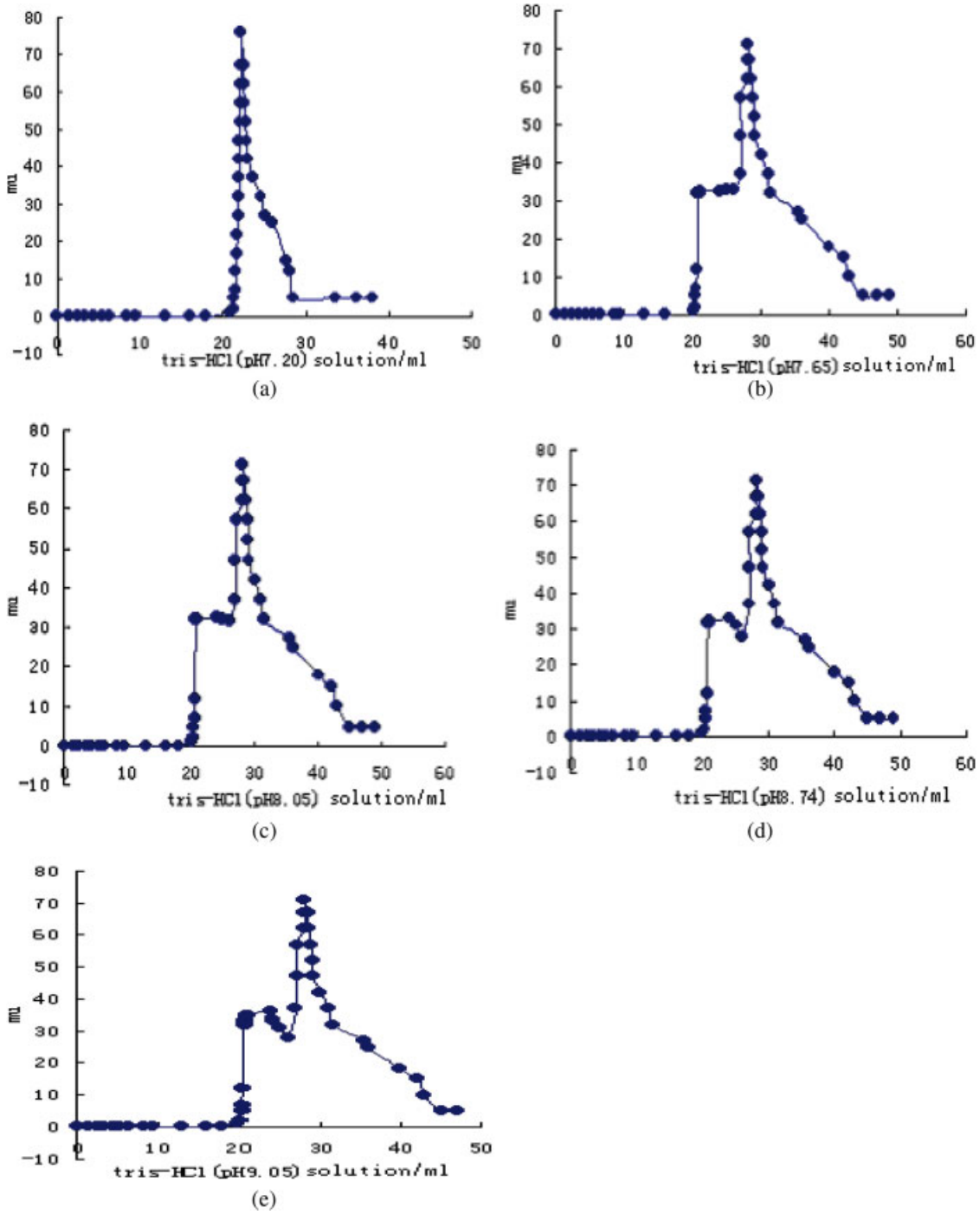

Figure 3 Effect of pH on eluent conditions. [Color figure can be viewed in the online issue, which is available at www.interscience.wiley.com.]

optimized system, ion strength, pH of the eluate, and the sizes of chitosan gel were selected to investigate their effects on elution conditions respectively.

Study of adsorption

About 1.0 g chitosan gel (125 μm, dry basis) was placed in a flask, into which 5.0 mL BSA solution was added. The mixture was shaken every 5 min. The aqueous samples were taken and analyzed with UV/visible spectrometer 751 (Shanghai, China) at 280 nm. To study the adsorption kinetics, 1.0 g chitosan gel (125 μm, dry basis) was first placed in a vessel, into which BSA solution was placed. The mixture was agitated. Samples were taken at the preset time interval. The amount of adsorption q_t at time t was calculated

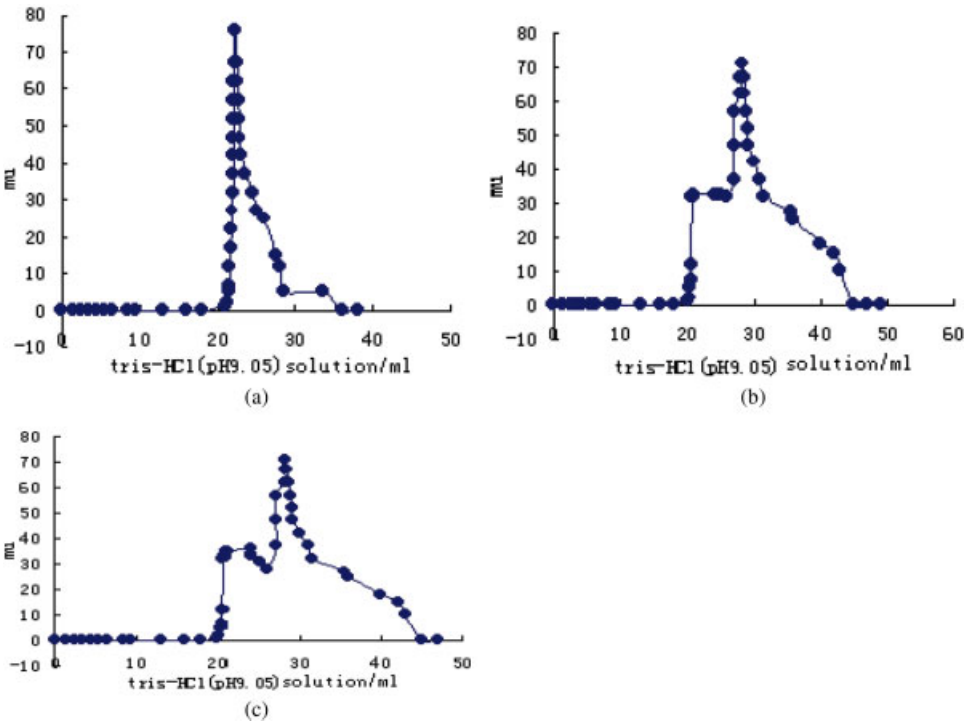

Figure 4 Effect of the sizes of gel on eluent conditions. The size of gel was (a) 80 μm, (b) 100 μm, and (c) 120 μm. [Color figure can be viewed in the online issue, which is available at www.interscience.wiley.com.]

by $q_t = (C_0 - C_t)$ (v/w), where C_t is the liquid concentration at any time.

IR measurement

The Infrared spectrum was measured on Nicolet 170SX Fourier transform IR spectrophotometer (USA). The spectrum was recorded with KBr pressed disk. The samples were chitosan, and chitosan adsorbed BSA.

Protein assay

Protein concentration was determined in accordance with the method of Folin–Loury.

RESULTS AND DISCUSSION

Determination of elution system

The results in Figure 1(a) show that when the eluent peak reached the highest it no longer dropped. What is more, the eluent volume was big in the system of baritone-HCl (pH, 9.0). Figure 1(b–e) shows that the elution profiles were similar, but they all had trailing phenomenon in the upper elution, which caused the increase of the eluent volume. The results shown in Figure 1(f), the peak was symmetric and the eluent volume was small. Thus Tris-HCl system was chosen as the elution system.

Optimization of elution conditions

Effect of ion strength on elution conditions

As shown in Figure 2, the elution peak had the trailing phenomenon with the increase in NaCl concentration. It might be because the hydrophobicity of gel was enhanced when Cl^- concentration was increased. But when *c* (NaCl) was 0.05 mol/L in Tris-HCl solution (pH, 9.05), it almost had no trailing phenomenon. The shape of the peak was good. Thus *c* (NaCl) 0.05 mol/L in Tris-HCl (pH, 9.05) was selected as eluent conditions.

Effect of pH on eluent conditions

The separation efficiency to BSA increased with the increase of pH, as shown in Figure 3. BSA could be divided into two peaks. With the increase of pH, the ionization of chitosan enhanced and the interval between pI and pH was bigger than before. Thus Tris-HCl (pH 8.0–9.0) was selected.

Effect of the sizes of gel on eluent conditions

As shown in Figure 4, with the decrease in chitosan gel sizes, the separation efficiency to BSA increased. But when 120–140 μm chitosan gel was used, the flow rate was too slow. From the angle of applications, chitosan gel (>120 μm) was selected.

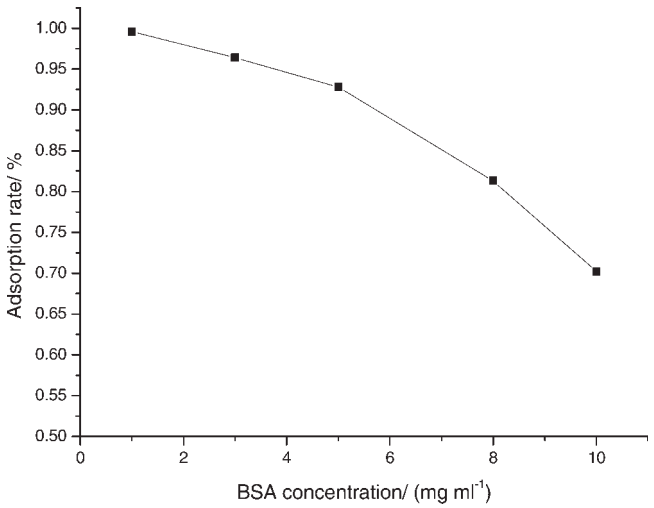

Figure 5 Effect of BSA concentration on adsorption.

Adsorption studies

Effect of BSA concentration and temperature on adsorption

Effect of BSA concentration and temperature on adsorption are presented in Figures 5 and 6. BSA adsorption rate increased from 70.2 to 99.6% as the adsorption temperature increased from 25 to 50°C at concentration of 5 mg/mL. The fact that the adsorption rate increased with the increase in temperature indicated the increase in the mobility of BSA molecules with increased temperatures, and the ongoing adsorption process was endothermic.[18,19] BSA concentrations 1, 3, 5, 8, 10 mg/mL were selected in this study. BSA adsorption rate decreased while BSA concentration was increased.

Effect of contact time on adsorption

Adsorption experiments were carried out for different contact times at 25°C with a fixed adsorbent dosage of 1.0 g. The results are presented in Figure 7. Similar plots were determined. BSA adsorption rate increased with the increase in contact time. The equilibrium time was 30 min. BSA adsorption rate was rapid in the initial stages of contact time and gradually increased with the increase in time until saturation. The adsorption curves were single, smooth, and continuous, indicating monolayer coverage of BSA on the outer interface of the adsorbent initially.[20]

Effect of pH on adsorption

The magnitude of electrostatic charges imparted by ionized BSA molecules was primarily controlled by medium pH. BSA adsorption rate tended to vary with aqueous medium pH.

The experimental results of BSA adsorption rate on chitosan gel as a function of pH at an initial BSA concentration of 5 mg/mL, temperature 25°C, and 1.0 g adsorbent dosage are shown in Figure 8. BSA adsorption rate increased from 53 to 82% with the increase in pH from 3 to 9. Maximum BSA adsorption rate was observed at pH 7.5, and beyond that pH it began to decrease. It was suggested that the increase in adsorption rate depended on the properties of the adsorbent surface and BSA structure.

Adsorption isotherms

The adsorption kinetics and sorption equilibrium were important criteria to the adsorbent. Many researchers have studied the adsorption isotherms of chitosan. Chitosan showed large adsorption capacity to chromium in pH 4.0 at 23°C.[21] Adsorption isotherms of BSA using chitosan gel at 25°C are presented in Figures 9–11.

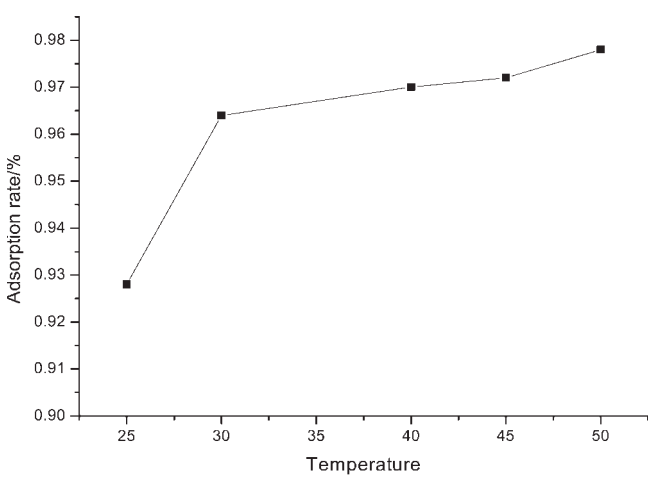

Figure 6 Effect of temperature on adsorption.

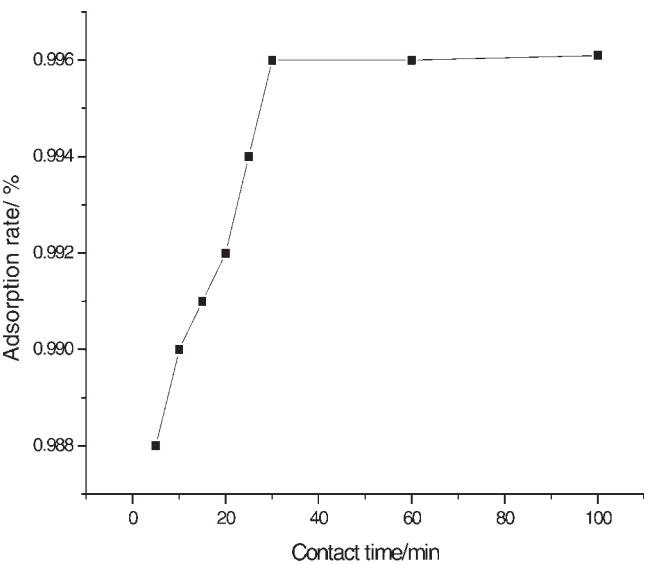

Figure 7 Effect of contact time on adsorption.

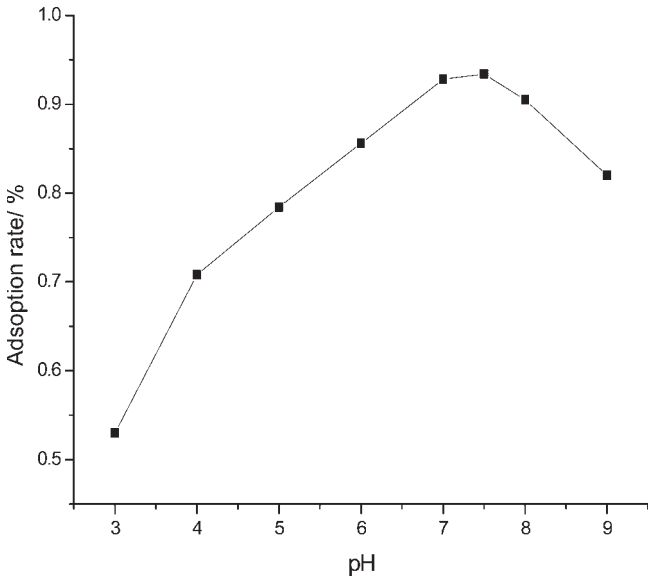

Figure 8 Effect of pH on adsorption.

Three theoretical isotherm models were used to fit the experimental data: Langmuir model, Freundlich model, and Redlich–Peterson model. Langmuir model was based on assumption homogeneity such as equally available adsorption site, monolayer surface coverage, and no interaction between adsorption species. The model was described by the following equation:

$$q = a\ K_L\ C_e/(1 + K_L C_e) \tag{1}$$

where q is the amount adsorbed at equilibrium time (mg/g), C_e was the equilibrium concentration (mg/mL), and a and K_L are the Langmuir coefficients related to adsorption capacity and energy of adsorption, respectively. Langmuir coefficients (a and K_L) could be calculated from the slope and intercept of the linearized plots of eq. (1). Weber and Chakraborti[22] proposed that Langmuir constant K_L could be expressed in terms of a dimensionless constant, separation factor (R_L), which was defined by

$$R_L = 1/(1 + K_L\ C_o) \tag{2}$$

where C_0 was the highest initial BSA concentration. As R_L value lay between 0 and 1, the on-going adsorption process was favorable. Further, R_L value for BSA was between 0 and 1 and therefore its adsorption was favorable.

Langmuir adsorption isotherm for BSA is shown in Figure 9. a represented the adsorption capacity when the surface was fully covered with BSA. a value was determined as 17.64 at 25°C for BSA. A high K_L value indicated the affinity for binding of BSA. The value of K_L was 0.53 found at 25°C for BSA. From the results shown in Figure 9, the adsorption was found to be well fitted to Langmuir model at 25°C.

The other well-known isotherm frequently used to describe adsorption behavior was Freundlich isotherm. This isotherm was another form of Langmuir approach for adsorption on a heterogeneous surface. The amount of adsorbed material was the summation of adsorption on all the sites. Freundlich isotherm described reversible adsorption and was not restricted to the formation of monolayer. This empirical equation takes the form

$$q = K_F(C_e)^{1/n} \tag{3}$$

where K_F and n are Freundlich constants characteristic of the system. The slope and the intercept of linear Freundlich equation were equal to $1/n$ and $1nK_F$ respectively. Figure 10 shows the plot of log q versus log C_e at 25°C. The plot is in harmony with Freundlich isotherm. One of the Freundlich constants K_F indicated the adsorption capacity of the adsorbent. The other Freundlich constant n was a measure of the deviation from linearity of the adsorption. If the value of n was equal to unity, the adsorption was linear. If the value of n was below unity, it implied that adsorption process was chemical, but if the value of n was above unity, adsorption was favorable, a physical process. The value of n at equilibrium, 2.63 at 25°C, represented favorable adsorption at high temperature.

The three-parameter Redlich–Peterson equation has been proposed to improve the fit by Langmuir or Freundlich equation and is given by eq. (4).

$$q = K_{RP}C_e/(1 + a_{RP}C_e^{\beta}) \tag{4}$$

where K_{RP}, a_{RP}, and β are the Redlich–Peterson parameters. β Lay between 0 and 1. For β = 1, Eq. (4)

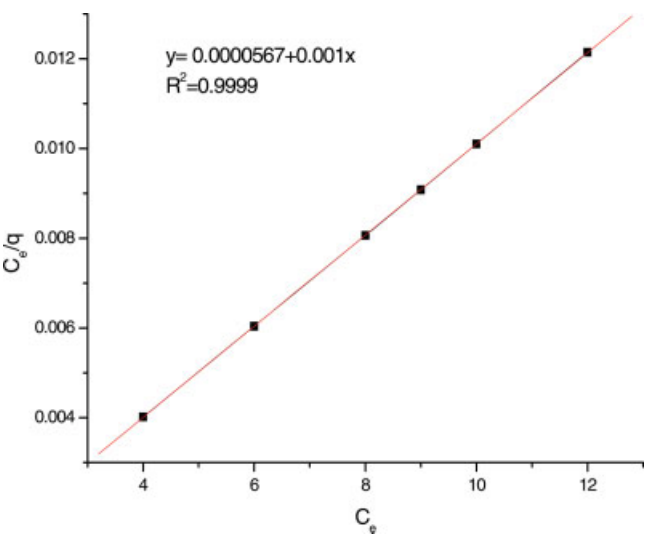

Figure 9 The plot of Langmuir model. [Color figure can be viewed in the online issue, which is available at www.interscience.wiley.com.]

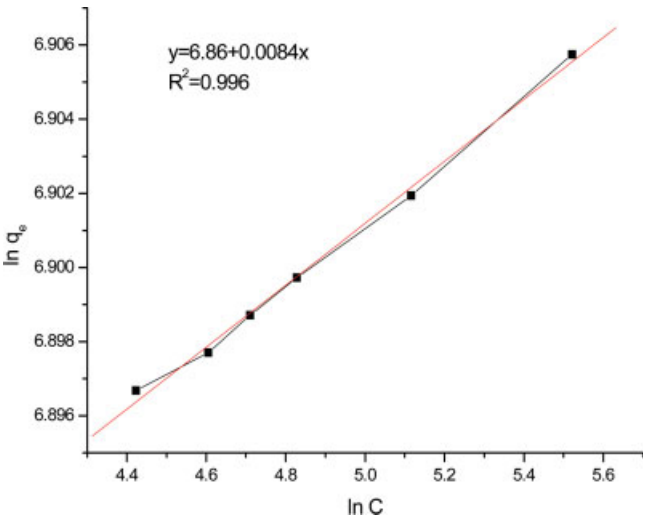

Figure 10 The plot of Freundlich model. [Color figure can be viewed in the online issue, which is available at www.interscience.wiley.com.]

was converted to Langmuir form. The adsorption model constants were obtained by nonlinear regression analysis method.

The experimental equilibrium data obtained from Redlich–Peterson adsorption model are presented in Figure 11. K_{RP} indicated the adsorption capacity of chitosan gel. The β value was found to be 1.0 for BSA.

From the above-mentioned discussion, it was evident that the surface of chitosan gel was made up of homogeneous and heterogeneous adsorption patches. In other words, all the isotherm models fitted very well when R^2 values were compared. Langmuir model correlation coefficient was 0.996, Freundlich model correlation coefficient was 0.999, and Redlich–Peterson model correlation coefficient was 0.956.

Adsorption kinetics

To investigate the controlling mechanism of adsorption such as mass transfer and chemical reaction, several kinetic models were used to test experimental data. First, the pseudofirst-order adsorption was used to test dynamical experimental data. The first-order rate expression of Lagergren was given as

$$\log(q - q_t) = \log(q) - k_1 t/2.3 \quad (5)$$

where q and q_t are the amounts of BSA adsorbed on the adsorbent at equilibrium and at time t respectively, and k_1 is the rate constant of first-order adsorption. The slope and intercepts of the plots of log $(q - q_t)$ versus t were used to determine the first-order rate constant k_1.

The pseudosecond-order equation was based on the adsorption equilibrium capacity and expressed in the form of

$$dq_t/dt = k_2(q - q_t)^2 \quad (6)$$

where k_2 is the rate constant of pseudosecond-order adsorption. Integrating this equation and applying the initial condition, we had $1/(q - q_t) = 1/q + k_2 t$ or equivalent to,

$$t/q + 1/k_2\ q^2 + t/q \quad (7)$$

It was observed that $k2$ and q could be calculated from the intercept and slope of the plot (t/q) versus t and there was no need to know any parameters in advance. Normally pseudofirst-order equation was expressed in the range of reaction only and did not fit well with the whole range of contact time and was generally applicable over the initial stage of the adsorption processes, although it has been effectively used to describe adsorption reactions.

The rate parameter for intraparticle diffusion was determined using the following equation:

$$q = k_{\text{int}} t^{1/2} + C \quad (8)$$

where C is the intercept and k_{int} is the intraparticle diffusion rate constant (mg/g $\text{min}^{1/2}$).

First, the values of log $(q - q_e)$ were calculated from the kinetic data in Figure 12. k_1 Values were calculated from the slope of this plot. In many cases the first-order equation of Lagergren did not fit well to the whole range of contact time and was generally applicable to the initial range of the adsorption process. The adsorption of BSA fitted to first-order of Lagergren k_1 was 15.63 h^{-1}.

Second, the plots of (t/q) versus t for the pseudosecond-order model given in eq. (7) are drawn in Figure 13.

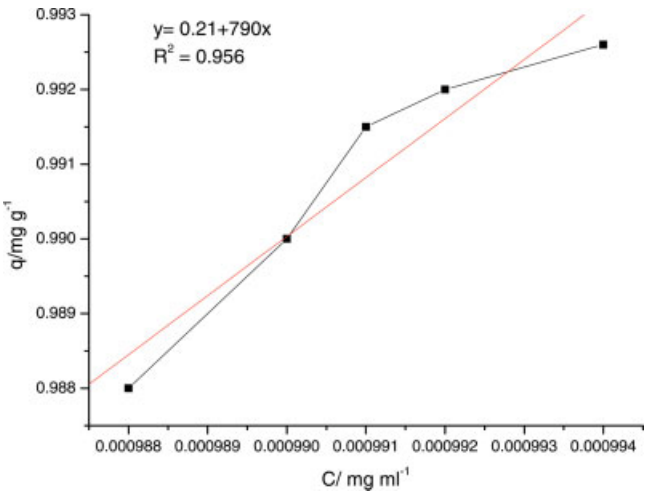

Figure 11 The plot of Redlich–Peterson model. [Color figure can be viewed in the online issue, which is available at www.interscience.wiley.com.]

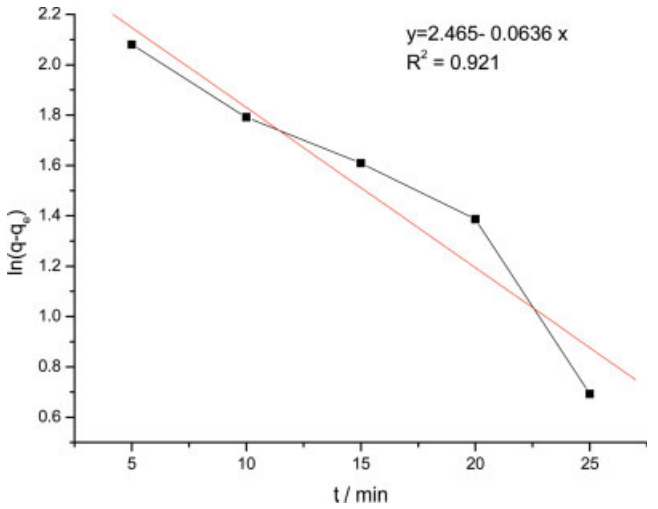

Figure 12 The pseudofirst-order adsorption of Lagergren equation. [Color figure can be viewed in the online issue, which is available at www.interscience.wiley.com.]

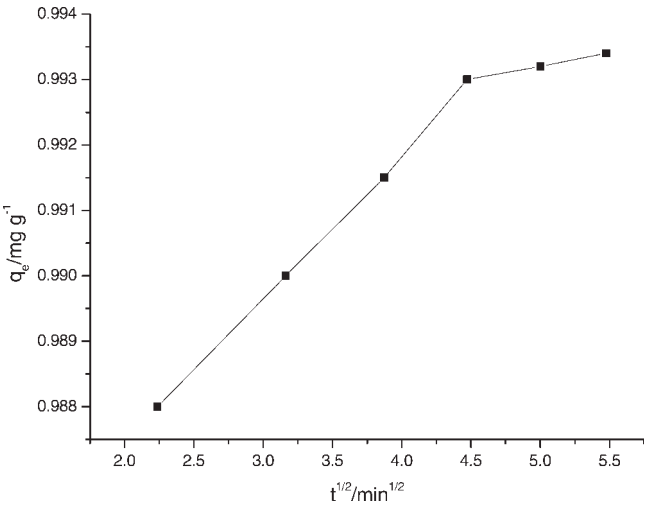

Figure 14 The plot of intraparticle model.

The q and k_2 values were 1000 and 0.011 calculated from slope and intercept of this plots, respectively.

Third, the intraparticle diffusion rate was obtained from the plots q versus $t^{1/2}$. The plots are shown in Figure 14: initial linear portion (Stage 1), followed by a plateau (Stage 2). The initial linear portion of this plot was attributed to intraparticle diffusion. k_{int} values were determined from the slope of initial linear portion of this plot. The value of intercept C gave an idea about the boundary layer thickness, i.e., the larger the intercept, the greater the boundary layer effect. The boundary layer diffusion depended on several parameters, including the external surface area of the adsorbent, which was mainly controlled by the particle size, the shape and density of the particles, the concentration of the solution, and the agitation velocity.

From the above-mentioned discussion, it is clear that the correlation coefficients of second-order kinetic model were greater than those of first-order kinetic model. These indicated that the adsorption perfectly complied with pseudosecond-order reaction.

The adsorption could be visualized using Avrami exponential function, which was an adaptation of kinetic thermal decomposition modeling,

$$\alpha = 1 - \exp[-k_{av}\ t]^n \tag{9}$$

where α is the adsorption fraction at time t, k_{av} is the adjusted kinetic constant, and n is another constant, which could be related to the adsorption mechanism. The linearized form of this equation is

$$\ln(-\ln(1-\alpha)) = n\ \ln\ k_{av} + n\ \ln\ t. \tag{10}$$

Figure 15 shows the general behavior of $\ln(-\ln(1-\alpha))$ versus $\ln\ t$ plots, in relation to the time. The numerical values of both angular and linear coefficients (data not shown) provided n and $\ln\ k_{av}$ values, respectively. The shapes of the curves suggested the presence of two linearized regions, in relation to the time. In this manner, two independent sets of values of n (n_1 to n_2) and k_{av} ($k_{av,1}$ to $k_{av,2}$) could also be considered. However, k_{av} values were related only to the adjustment of the kinetic data, and their values did not reflect the adsorption kinetic constants. So the most important factor in Avrami kinetic model was the constant n, the values of which could be used to verify possible alterations of the adsorption mechanisms in relation to contact time and temperature. For BSA, the values of n_1 and n_2 were 0.062 and 0.32 respectively. The higher values of n_2 suggested that

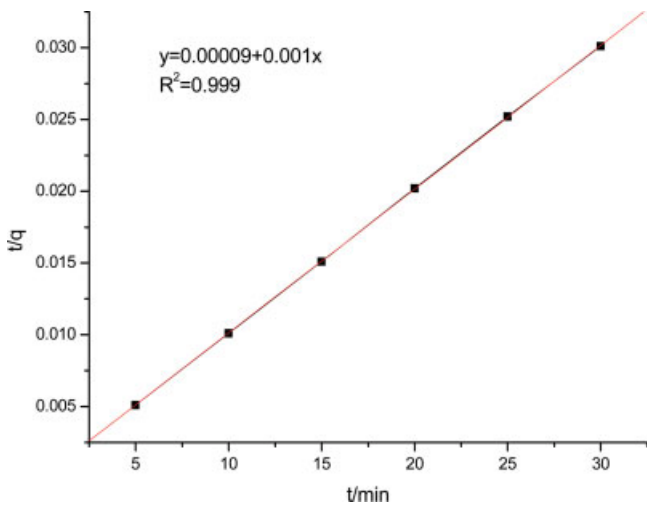

Figure 13 The pseudosecond-order adsorption of Lagergren equation. [Color figure can be viewed in the online issue, which is available at www.interscience.wiley.com.]

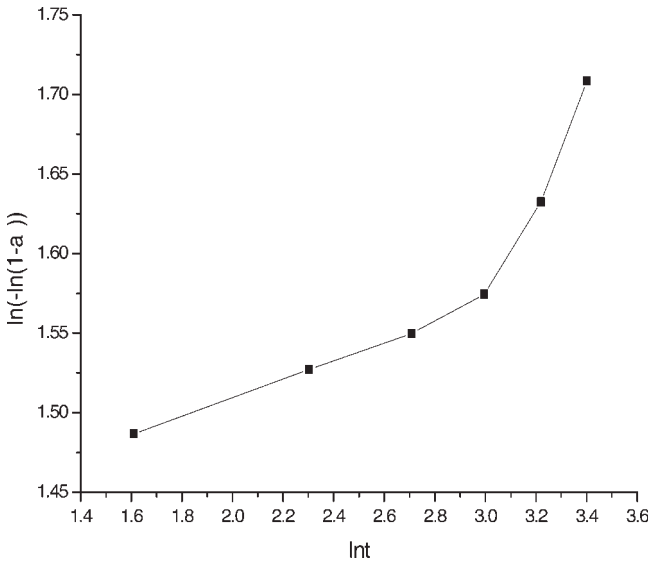

Figure 15 The plot of Avrami.

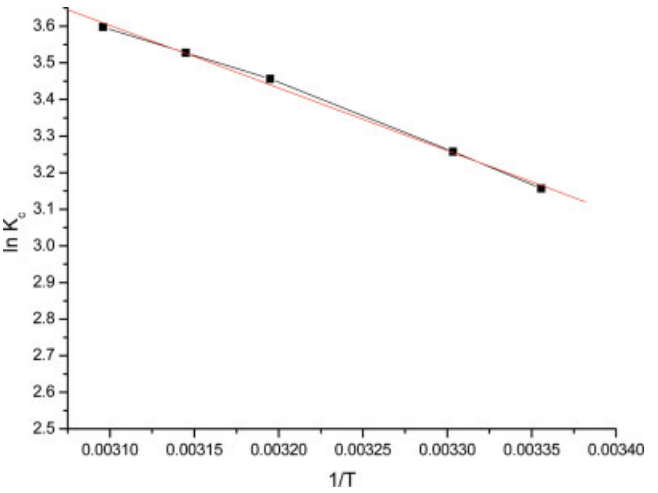

Figure 16 The plot of van't Hoff. [Color figure can be viewed in the online issue, which is available at www.interscience.wiley.com.]

the diffusion of BSA was faster than the mass transfer processes.

Adsorption thermodynamics

Effect of concentration and temperature on BSA adsorption are shown in Figures 5 and 6. When the temperature was increased, adsorption rate increased slightly. The change in standard free energy (ΔG°), enthalpy (ΔH°), and entropy (ΔS°) of adsorption were calculated from the following equation:

$$\Delta G^\circ = -RT \ln K_c \tag{11}$$

where R is the gas constant, K_c is the equilibrium constant, and T is the temperature (K). K_c value was calculated from eq. (12)

$$K_c = C_{Ae}/C_{Se} \tag{12}$$

where C_{Ae} and C_{Se} are the equilibrium concentration of BSA on adsorbent (mg/mL) and in the solution (mg/mL) respectively. Standard enthalpy (ΔH°) and entropy (ΔS°) of adsorption could be estimated from van't Hoff equation given as

$$\ln K_c = -\Delta H^\circ_{ads}/RT + \Delta S^\circ/R \tag{13}$$

The slope and intercept of the van't Hoff plot was equal to $-\Delta H^\circ_{ads}/R$ and $\Delta S^\circ/R$, respectively. The van't Hoff plot of the BSA adsorption is given in Figure 16. Thermodynamic parameters obtained are summarized in Table I.

It can be seen in Table I that ΔH° value was 14.22 kJ/mol. The positive value of enthalpy change conformed to the endothermic nature of the adsorption process. The positive value of ΔS° reflected the affinity of adsorbent material towards BSA. The entropy (ΔS°) value was 74.04 J/mol K. Despite being endothermic in nature, the spontaneity of the adsorption process was decreased in Gibbs energy of the system. ΔG° values varied in range, with the values showing a gradual increase from −7.82 to −9.33 kJ/mol at 25°C in accordance with the endothermic nature of the adsorption process.

IR spectrum studies

The infrared spectra of chitosan-adsorbed BSA (Fig. 17) were investigated and the compared experiments were carried out with chitosan (Fig. 18).

The results indicated that an obvious change took place after the adsorption. A weak band in the region of 1654 cm^{-1} (δ_{NH} of NH_2 group) was observed, which indicated 2′ NH_2 group had been taken into the adsorption. There was no obvious adsorption at about 2120–2185 cm^{-1} (due to C=N). A band in the region of 1036 cm^{-1} (Fig. 17) and 1066 cm^{-1} (Fig. 18) were moved toward higher wavenumbers about 25 and 5 cm^{-1} respectively. It might be the adsorption site.

TABLE I
Thermodynamic Parameters for the Adsorption of BSA on Chitosan Gel

Temperature (°C)	K_c	$-\Delta G$ (kJ/mol)	ΔH (kJ/mol)	ΔS (J/mol K)
25	12.89	7.82	14.22	74.039
30	26.79	8.21		
35	32.33	8.99		
40	34.71	9.33		
45	44.45	9.66		

Concentration, 5 mg/mL.

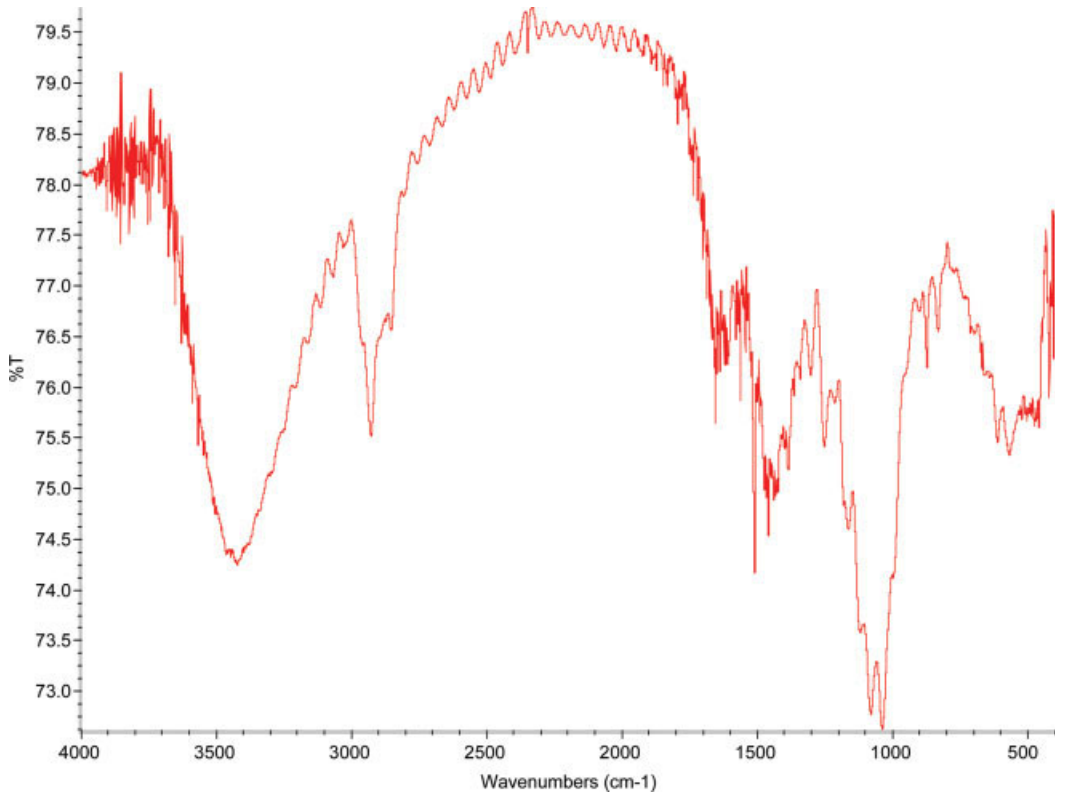

Figure 17 IR of chitosan-adsorbed albumin bovine serum. [Color figure can be viewed in the online issue, which is available at www.interscience.wiley.com.]

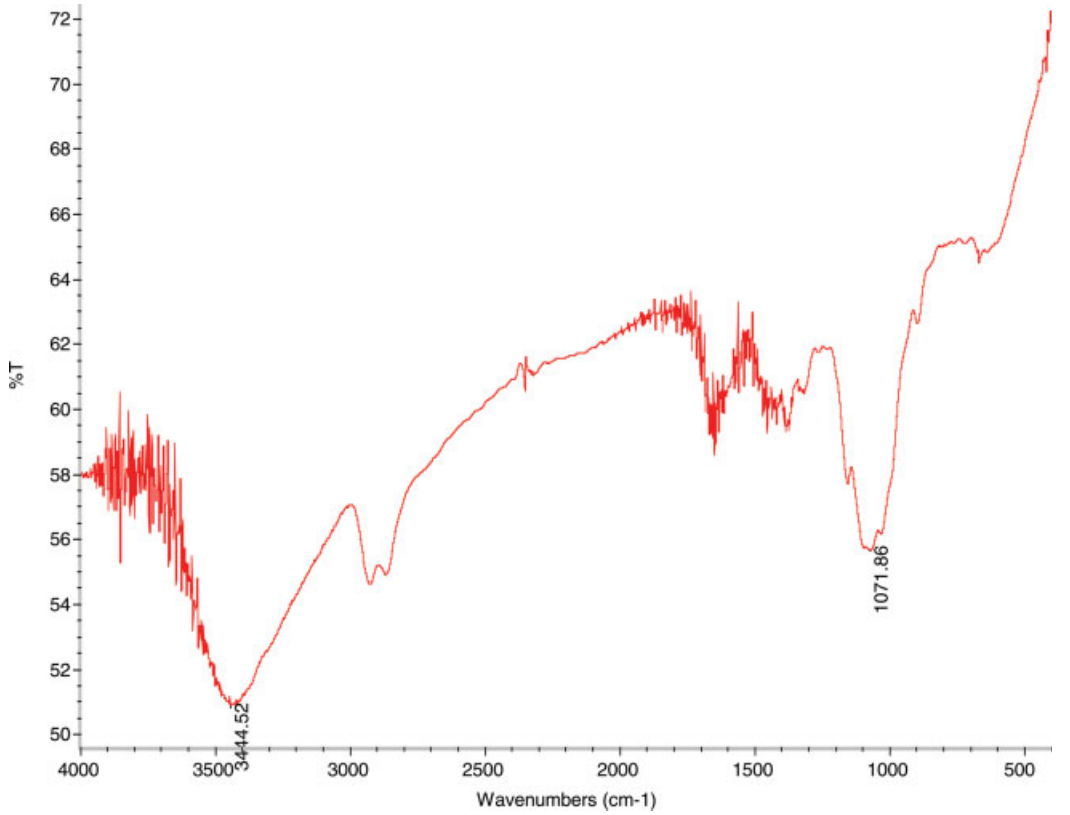

Figure 18 IR of chitosan. [Color figure can be viewed in the online issue, which is available at www.interscience.wiley.com.]

CONCLUSIONS

Chitosan had many excellent chemical properties like sepharose, such as chemical stability and compatibility with bioactive compounds. So it was possible to be used as gel carrier. The best elution system was Tris-HCl (pH, 9.05). Particle size of chitosan gel was 120–140 μm. The elution conditions were c (NaCl) = 0.05 mol/L in Tris-HCl (pH, 9.05) at a flow rate of 2.0–3.0 mL/min.

The ability of chitosan gel to adsorb BSA was investigated in the batch system. It was seen that initial pH, temperature, contact time, and initial BSA concentration highly affected the adsorption capacity of the sorbent. The equilibrium of adsorption of BSA onto chitosan gel was tested using Langmuir, Freundlich, and Redlich–Peterson models. Although all the adsorption models applied agreed well with the experimental data, Lagergren model, intraparticle diffusion model, and Avrami model gave good fit to experimental results. Thermodynamic constants were also evaluated using equilibrium constants with changed temperature. The negative value of ΔG° indicated the spontaneity of the process. The positive values of ΔH° and ΔS° showed the endothermic nature and irreversibility of BSA adsorption.

There were two hydrogens in amino group, which might shape two hydrogen bonds, hindering the curve wave of amino group. In the region of 1654 cm^{-1}, its strength took change in spite of the position unchanged. It might be an adsorption site. OH group might shape hydrogen bond between amino group and protein, which might be the other adsorption site. During the adsorption of BSA, the region of 1654 cm^{-1} adsorption might be the mainly adsorption site.

References

1. Robert, G. A. F. Chitin Chemistry. MacMillan: London, 1992.
2. Holme, K. R.; Hall, L. D.; Armstrong, C. R.; Withers, S. G. Carbohydr Res 1988, 173, 285.
3. Sentsad, C.; Mattiasson, B. Biotechnol Bioeng 1989, 33, 216.
4. Shi, Y. C.; Jiang, Y. M.; Sui, D. X.; Li, Y. L.; Chen, T.; Ma, L.; Ding, Z. T. J Chromatogr A 1996, 742, 107.
5. Muzzarelli, R. A. A.; Tanfani, F. Pure Appl Chem 1982, 54, 2141.
6. Inoue, K.; Baba, Y.; Yoshizuka, K. Bull Chem Soc Jpn 1993, 66, 2915.
7. Domard, A. Int J Biol Macromol 1987, 9, 98.
8. Guibal, E.; Milot, C.; Roussy, J. Sep Sci Technol 2000, 35, 1021.
9. Piron, E.; Domard, A. Int J Biol Macromol 1997, 21, 327.
10. Guibal, E.; Milot, C.; Tobin, J. M. Ind Eng Chem Res 1998, 37, 1454.
11. Juang, R. S.; Ju, C. Y. Ind Eng Chem Res 1998, 37, 3463.
12. Jha, I. N.; Iyengar, L.; Prabhakara Rao, A. V. S. J Environ Eng 1988, 114, 962.
13. Gonzalez-Davila, M.; Santana-Casiano, J. M.; Millero, F. J. J Colloid Interface Sci 1990, 137, 102.
14. Rorrer, G. L.; Hsien, T. Y.; Way, J. D. Ind Eng Chem Res 1993, 32, 2170.
15. Weltrowski, M.; Martel, B.; Morcellet, M. J Appl Polym Sci 1996, 59, 647.
16. Inoue, K.; Hirakawa, H.; Ishikawa, Y.; Yamaguchi, T.; Nagata, J.; Ohto, K.; Yoshizuka, K. Sep Sci Technol 1996, 31, 2273.
17. Kaminski, W.; Modrzejewska, Z. Sep Sci Technol 1997, 32, 2659.
18. Acemioğlu, B. J Colloid Interface Sci 2004, 274, 371.
19. Mittal, A.; Krishnan, L.; Gupta, V. K. Sep Purif Technol 2005, 43, 125.
20. Namasivayam, C.; Thamaraiselvi, K.; Yamuna, R. T. Pest Sci 1994, 41, 7.
21. Udaybhaskar, P. J Appl Polym Sci 1990, 39, 739.
22. Weber, T. W.; Chakraborti, R. K. AIChE J 1974, 20, 228.